Information Content of Limb Radiances from MIPAS

Anu Dudhia

Atmospheric, Oceanic and Planetary Physics
University of Oxford, Oxford, UK

1 Introduction

1.1 Nadir v. Limb Spectra

Fig. 1 illustrates the main differences between nadir sounding and limb sounding infrared measurements.

Nadir views have the relatively warm background of the earth's surface or lower troposphere, while limb views have the cold background of space. Consequently, spectral signatures of gases in the nadir view generally appear as absorption features bounded by the the 'Brightness Temperature' curves corresponding to the Planck function for the highest and lowest temperatures along the path. In the limb view, the usual appearance is as emission features with radiances covering the full range from zero to atmospheric temperatures. Apart from the strong CO_2 and O_3 bands, limb radiances are typically orders of magnitude smaller, so often requiring longer integration times for adequate S/N. However, while much of the nadir spectrum is dominated by H_2O features, the relatively dry stratosphere allows signatures of other gases to be more clearly distinguished.

1.2 MIPAS

The Michelson Interferometer for Passive Atmospheric Sounding (ESA, 2000) was launched on ESA's Envisat satellite on 1st March 2002. MIPAS is a Fourier transform spectrometer with a maximum optical path difference of 20 cm, giving spectra sampled at 0.025 cm^{-1} (actual resolution is closer to 0.035 cm^{-1}), split into 5 bands in the range 685–2410 cm^{-1} (14.5–4.1 μm). MIPAS views the atmospheric limb with a field-of-view approximately 3 km high $\times$ 30 km wide. Usually viewing is in the rearward direction although it also has the capability to view sideways. In the nominal observing mode, a spectrum is acquired every 4.6 seconds at each of 17 tangent altitudes starting at 68 km and finishing at 6 km (3 km steps between 42–6 km). A complete limb scan is obtained approximately every 80 seconds, or 500 km along-track (Fig.2), giving over 1000 profiles a day.

MIPAS operated in nominal mode from July 2002 until March 2004 when it was switched off following increasingly frequent problems with the interferometer slide mechanism. There are plans to reactivate the instrument towards the end of 2004 using a slide movement reduced by a factor 2.5, hence a wider spectral sampling of 0.0625 cm^{-1}.

2 MIPAS Retrievals

2.1 ESA Processing

The European Space Agency retrieves profiles of temperature and the composition, 'Level 2 Data', on an operational basis (Table 1). As with most limb sounding, it is also necessary to retrieve the tangent point pressure

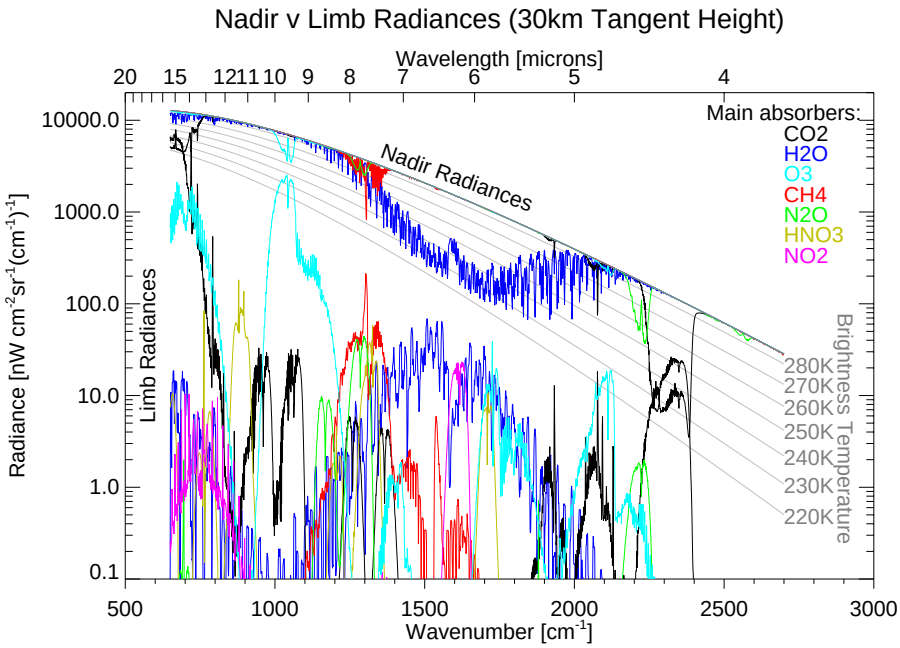

Figure 1: Comparison of mid-infrared spectra for the same atmosphere for a nadir-view and a limb-view at 30km tangent height, showing the spectral features of the major contributing gases.

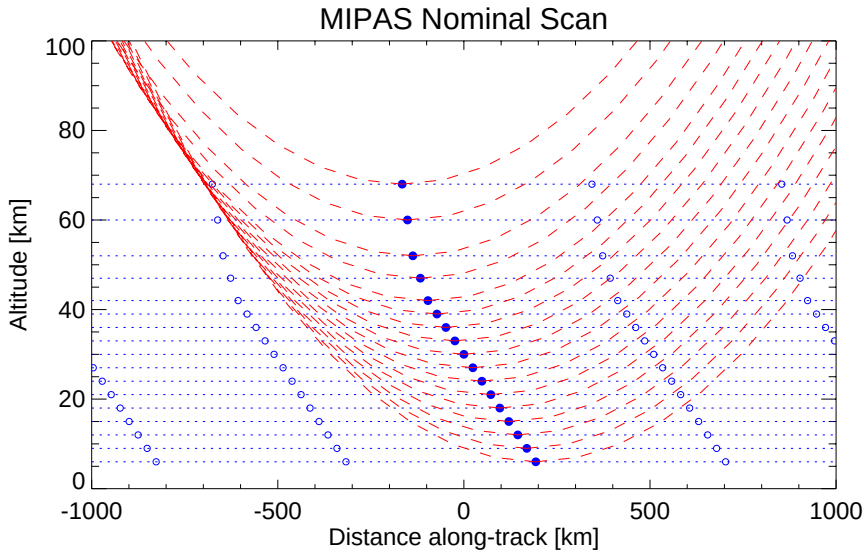

Figure 2: The tangent paths (dashed red lines) and tangent points (solid blue circles) for a nominal MIPAS rear-viewing limb scan, with the satellite to the right and moving right. Open circles show tangent points from successive scans.

which is performed jointly with the temperature retrieval. The *pT* retrieval is followed by the sequential retrieval of H_2O, O_3, HNO_3, CH_4, N_2O and NO_2, the order being such that the major absorbers are retrieved first so that their spectral interference within the features of the minor absorbers can be better modelled.

There are actually two versions of ESA's L2 data: the *Near Real Time* (NRT) products, generated within a few hours of acquisition, and the *Off-Line* products which are generated within a few weeks. In theory the

Off-Line data is more accurate since it benefits from better calibrated spectra and more CPU time (e.g., using tighter retrieval convergence criteria), however the most obvious difference is the extended altitude range of the Off-Line data.

Table 1: Altitude ranges of the MIPAS L2 profiles generated by ESA (lower altitude assumes a cloud-free scene).

Species	Near Real Time	Off-Line
pT	12–68 km	6–68 km
H_2O	12–60 km	6–68 km
O_3	12–60 km	6–68 km
HNO_3	12–42 km	9–42 km
CH_4	12–60 km	6–68 km
N_2O	12–47 km	6–60 km
NO_2	24–47 km	24–68 km

There have been several modifications to the processing software during MIPAS operations, the most significant being the introduction of cloud detection in July 2003. The Off-Line data is currently being reprocessed with the latest software version (v4.61).

2.2 Microwindows

The measurement domain for a spectrally resolving limb sounder can be considered to be a two-dimensional grid of tangent altitude v. spectral channel. In principle it is possible to use individual measurements within this domain however it is more common to use 'microwindows': rectangular subsets of adjacent measurements. The main reason is to allow a spectrally flat atmospheric continuum absorption term to be retrieved (and therefore eliminated) within each microwindow. Forward models, which generally form the major part of the computational effort for a retrieval, also benefit from efficiencies e.g., when convolving in the spectral domain to model the instrument line shape, or the tangent height domain to model the field of view. A further advantage when using an microwindow selection scheme such as outlined here, is that the continuum retrieval provides additional flexibility in absorbing or cancelling systematic errors (assuming that an accurate continuum retrieval is not itself a requirement).

Fig. 3 shows the locations of the microwindows used for the Off-Line retrievals. Since each species is retrieved separately, the microwindows are positioned to select spectral regions where the lines of the target molecule dominate (CO_2 in the case of the pT retrieval).

2.3 Retrieval Algorithm

The ESA retrieval algorithm (Ridolfi *et al*, 2000) is non-linear 'Least Squares Fit' which, in linearised form, may be represented as the minimisation of the cost function:

$$\chi^2 = (\mathbf{y} - \mathbf{K}\mathbf{x})^T \mathbf{S}_y^{-1} (\mathbf{y} - \mathbf{K}\mathbf{x}) \tag{1}$$

where $\mathbf{y}$ is the set of measurements with noise covariance $\mathbf{S}_y$, $\mathbf{x}$ is the state vector (i.e., profile to be retrieved) and $\mathbf{K}$ the *Jacobian* (or *Weighting Function*) matrix with elements $K_{ij} = \partial y_i / \partial x_j$.

This has the standard solution (e.g., Rodgers, 2000)

$$\mathbf{x} = \mathbf{G}\mathbf{y} \tag{2}$$

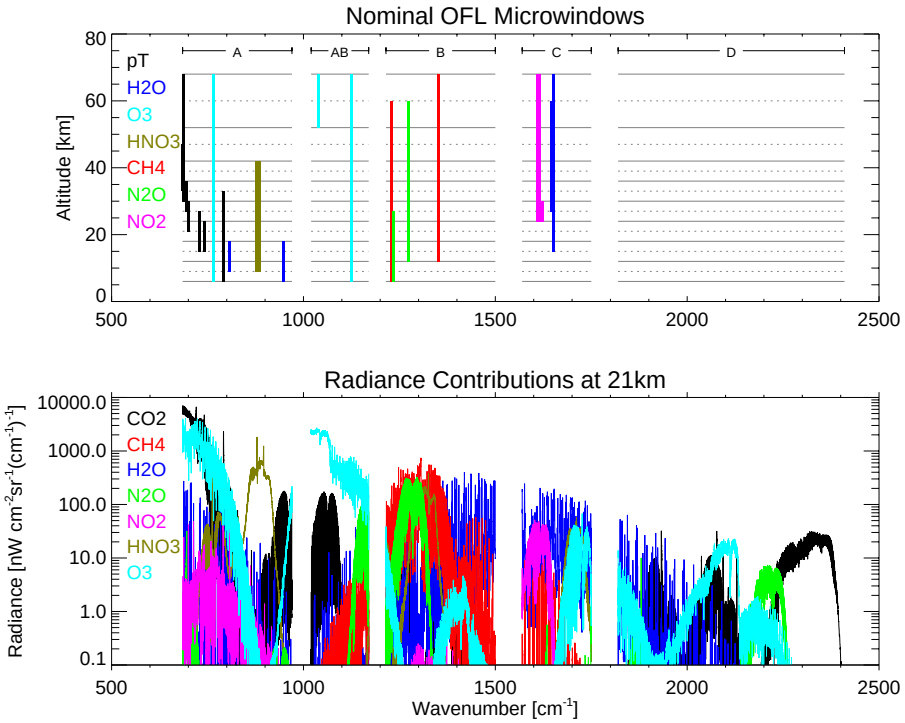

Figure 3: The upper plot shows the major absorbing molecules in the MIPAS spectra for 21km tangent altitude and the lower plot shows the spectral locations and tangent altitude range of the microwindows used for the MIPAS Off-Line retrievals (note that the actual spectral width of each microwindow — maximum 3 cm^{-1} — is too narrow to be shown to scale on these plots).

where $\mathbf{G}$ is the *Gain* (or *Contribution Function*) matrix with elements $G_{ji} = \partial x_j / \partial y_i$ given by

$$\mathbf{G} = \left(\mathbf{K}^T \mathbf{S}_y^{-1} \mathbf{K}\right) \mathbf{K}^T \mathbf{S}_y^{-1} \tag{3}$$

Therefore it follows that the solution covariance $\mathbf{S}_x$ is related to the measurement covariance $\mathbf{S}_y$ by

$$\mathbf{S}_x = \mathbf{G}\mathbf{S}_y\mathbf{G}^T \tag{4}$$

$$= \left(\mathbf{K}^T \mathbf{S}_y^{-1} \mathbf{K}\right)^{-1} \tag{5}$$

2.4 Total Error

The ESA retrieval assumes a Gain matrix $\mathbf{G}$ based only on the random noise component of measurement error $\mathbf{S}_y \equiv \mathbf{S}_y^{\mathrm{rnd}}$. The noise in adjacent spectral channels is assumed to be uncorrelated, but since the retrieval uses apodised spectra, the smoothing effect of the apodisation is accounted for in the off-diagonal elements of $\mathbf{S}_y^{\mathrm{rnd}}$.

However, there are a number of additional sources of (systematic) error (Table 2) either in measurements or in the forward model which, although not modelled in the retrieval itself, can be modelled retrospectively as additional independent error components $\mathbf{S}_y^i$ giving a *total measurement error* covariance:

$$\mathbf{S}_y^{\mathrm{tot}} = \mathbf{S}_y^{\mathrm{rnd}} + \sum_i \mathbf{S}_y^i \tag{6}$$

Following the form of Eq. 4, this gives a *total retrieval error* covariance:

$$\mathbf{S}_x^{\mathrm{tot}} = \mathbf{G}\mathbf{S}_y^{\mathrm{rnd}}\mathbf{G}^T + \mathbf{G}\left(\sum_i \mathbf{S}_y^i\right)\mathbf{G}^T \tag{7}$$

Table 2: MIPAS error sources, in addition to random noise ('Code' refers to key in Fig. 4).

Error Source	$1\,\sigma$	Code
Errors in Instrument Characterisation		
Radiometric Gain	±2%	GAIN
Spectral Calibration	$\pm 0.001\text{cm}^{-1}$	SHIFT
Apodised ILS Width	±2%	SPREAD
Errors in Forward Model Parameters		
Profiles of 28 gases	Climat.SD	[gas]
High Alt. Column	Climat.SD	HIALT
Line database errors	[1]	SPECDB
Continuum model	±25%	CTMERR
Retrieved p error	±2% [2]	PRE
Retrieved T error	±1 K [2]	TEM
Deficiencies in Forward Model		
Non-LTE effects	Modelled	NONLTE
CO_2 Line Mixing	Modelled	CO2MIX
Horiz.T gradients	±1K/100km	GRA

[1] Based on assumed 1σ accuracies in line position, strength and halfwidth
[2] Impact of pT retrieval errors on subsequent constituent retrievals

$$= \mathbf{S}_x^{\text{rnd}} + \sum_i \mathbf{S}_x^i \tag{8}$$

$$= \mathbf{S}_x^{\text{rnd}} + \mathbf{S}_x^{\text{sys}} \tag{9}$$

Note that the definition of $\mathbf{G}$ itself (Eq. 3, with $\mathbf{S}_y \equiv \mathbf{S}_y^{\text{rnd}}$) is unchanged since this is fixed by the retrieval algorithm.

The square roots of the diagonal elements of terms in Eq. 9 for the MIPAS temperature retrieval are shown in Fig. 4.

3 Microwindow Selection

3.1 Information Content

Measurements, or microwindows, can be selected to maximise some scalar parameter, or 'Figure of Merit', describing the quality of the retrieval. One possible such parameter is the the *(Shannon) Information Content*, H, defined as:

$$H = -\frac{1}{2}\log_2 \left|\mathbf{S}_x \mathbf{S}_a^{-1}\right| \tag{10}$$

where $\mathbf{S}_x$ is the retrieval (or *a posteriori*) covariance, $\mathbf{S}_a$ is the *a priori* covariance and $|\ldots|$ indicates the determinant. H is measured in bits. In simple terms, if the retrieval reduces the variance at one profile level by a factor 4 (i.e., a factor 2 in standard deviation) this corresponds to 1 bit of information.

There is no explicit *a priori* estimate in the ESA retrieval although we can define the information in terms of an improvement over a 'climatological' covariance $\mathbf{S}_a$, e.g., a diagonal matrix with elements $(10\text{ K})^2$ for

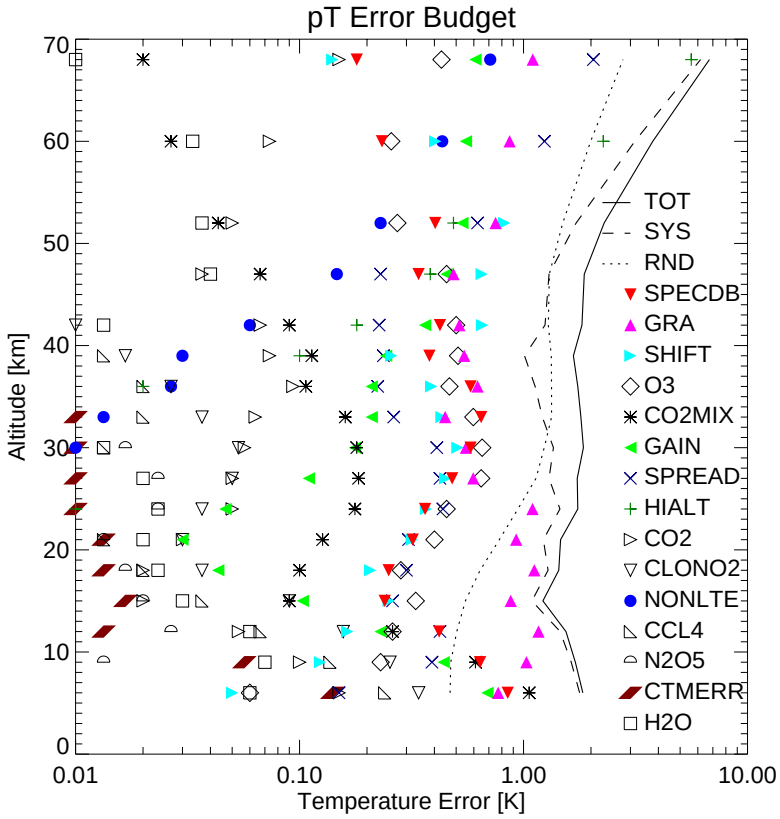

Figure 4: Error budget for the temperature component of the MIPAS Off-Line pT retrieval computed for mid-latitude day-time conditions. The solid line is the Total Error (or Accuracy), represented by the root-sum-square of the Random Error (or Precision), shown as the dotted line, and the Systematic Error, shown as the dashed line. The Systematic Error is itself the root-sum-square of the various components shown by different symbols (see Table 2 for details).

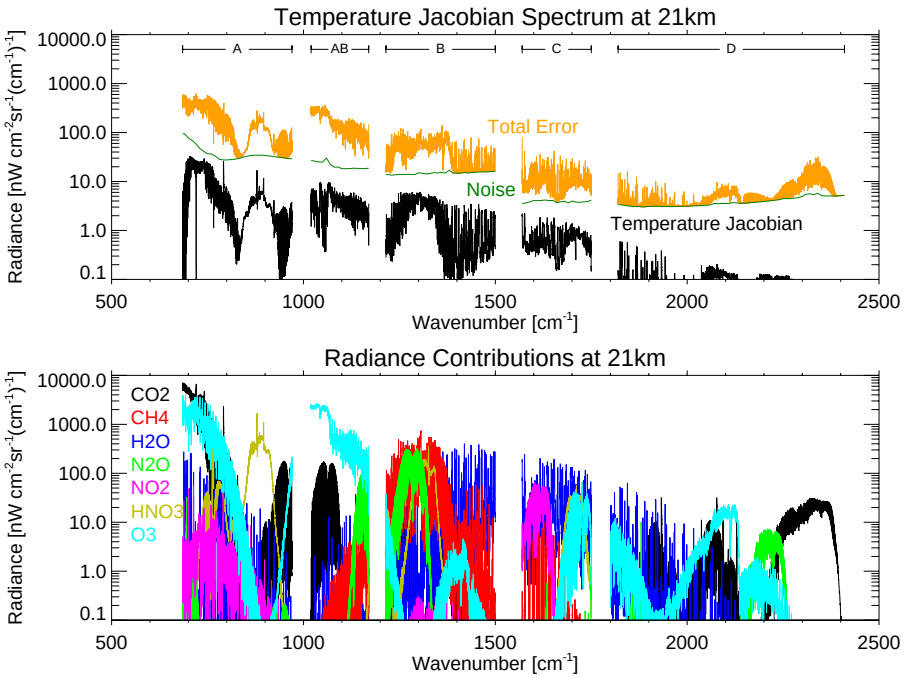

Figure 5: Illustration of the difference between selecting temperature channels based on Noise or Total Error considerations, considering the 21km tangent altitude. For the former, the best channels are those which maximise the ratio of the Temperature Jacobian (in black) to the Noise (green). For the latter it is the ratio of the Temperature Jacobian to the Total Error (orange), which weights the selection towards regions where the concentration of the major emitting species is well-known (i.e., CO_2).

temperature. However, this means that the absolute value of the information content of the MIPAS retrieval is somewhat arbitrary.

There is the issue as to whether the retrieval covariance $\mathbf{S}_x$ in Eq. 10 should represent just the random error covariance $\mathbf{S}_x^{\mathrm{rnd}}$ or total error covariance $\mathbf{S}_x^{\mathrm{tot}}$ from Eq. 9 (it is assumed that the *a priori* covariance $\mathbf{S}_a$ is purely random). If only the random (noise) error is considered, the best channel is effectively that which maximises the ratio of sensitivity ($\sim\mathbf{K}$, the Jacobian) to noise ($\sim\sqrt{\mathbf{S}_y^{\mathrm{rnd}}}$). Fig. 5 demonstrates the problem with this approach: while the noise spectrum is smooth, the temperature Jacobian is broadly similar to the overall radiance spectrum itself, with no distinction between CO_2 features and those of other gases with variable concentrations.

One could manually restrict the channels to consider only those for which CO_2 is the dominant absorber but a better solution is to consider the total error, in which case the measurement error includes not only the noise but systematic errors such uncertainties in modelling profile concentrations of the different species.

3.2 Selection Algorithm

The MIPAS microwindow selection algorithm is described in detail in Dudhia *et al.* (2002). Basically, the method is to find the single measurement which contributes the most information and then 'grow' a microwindow by adding adjacent points (in both the spectral and tangent altitude domains) until either the maximum allowed size is reached (i.e., 3cm^{-1} width and all 17 tangent altitudes) or adding any further points results in a loss of information.

The retrieval total error covariance after incorporating this first microwindow then replaces the *a priori* covariance in Eq. 10 and the process repeated to find the second best microwindow, etc.

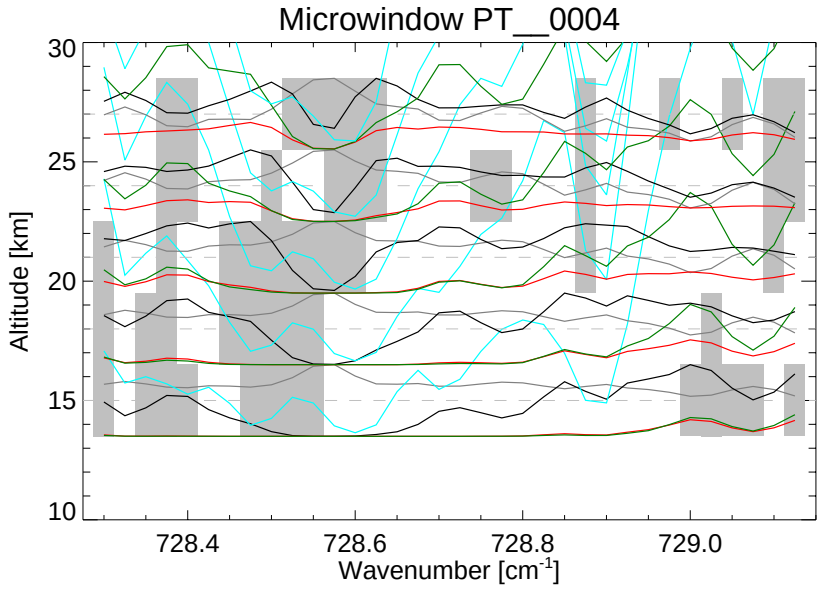

Figure 6: One of the pT microwindows used in the operational MIPAS retrieval. The black curves show the temperature Jacobian spectra (1K perturbation) at each tangent altitude, and on the same scale the red curves the pressure Jacobians (1%) , the green curves the continuum extinction Jacobians ($10^{-4} km^{-1}$) and the blue curves the radiance contribution from the uncertainty in O_3 concentration. On a different scale, the grey curve shows the overall shape of the spectra. The grey boxes indicated which measurements are masked out at each altitude.

The retrieval Gain matrix is assumed to weight measurements only by the random noise component. A consequence of this is that, while the random component of error can only *decrease* as further measurements are added, it is possible that the total error can *increase* if the measurement introduces a systematic error which outweighs the random error reduction. That is, some measurements have 'negative' information. As the microwindow boundaries are expanded, the selection algorithm allows such measurements to be flagged for exclusion from the retrieval, applying a so-called 'spectral mask'.

Fig. 6 shows one of the operational *pT* microwindows include positions of masked measurements. In this plot, although there may be some tendency to mask out the centres of saturated lines (indicated by regions where the Jacobians are low but the overall radiance is high) to avoid problems with horizontal temperature gradients, the general positioning of masks is non-obvious and bears little relation to the location, for example, to the spectral points most affected by uncertainties in the concentration of the major interfering gas for this region, ozone. This is a consequence of a selection algorithm which optimises for the full retrieval rather than individual tangent heights in single microwindows, which is how the human eye perceives the problem.

3.3 Limiting Accuracy

Considering only the random component, then every spectral point would contribute to the *pT* retrieval precision (if not positively, at least not negatively) so eventually microwindows would be selected covering the complete spectrum. However, considering the total error, another consequence of the non-optimal weighting and associated negative information weighting is that there will be only a limited number of useful microwindows within a spectrum.

To illustrate this, a simplified form of the MIPAS microwindow selection algorithm has been used to select the first 100 of a sequence of microwindows for a *pT* retrieval. Fig. 7 shows the locations of these microwindows.

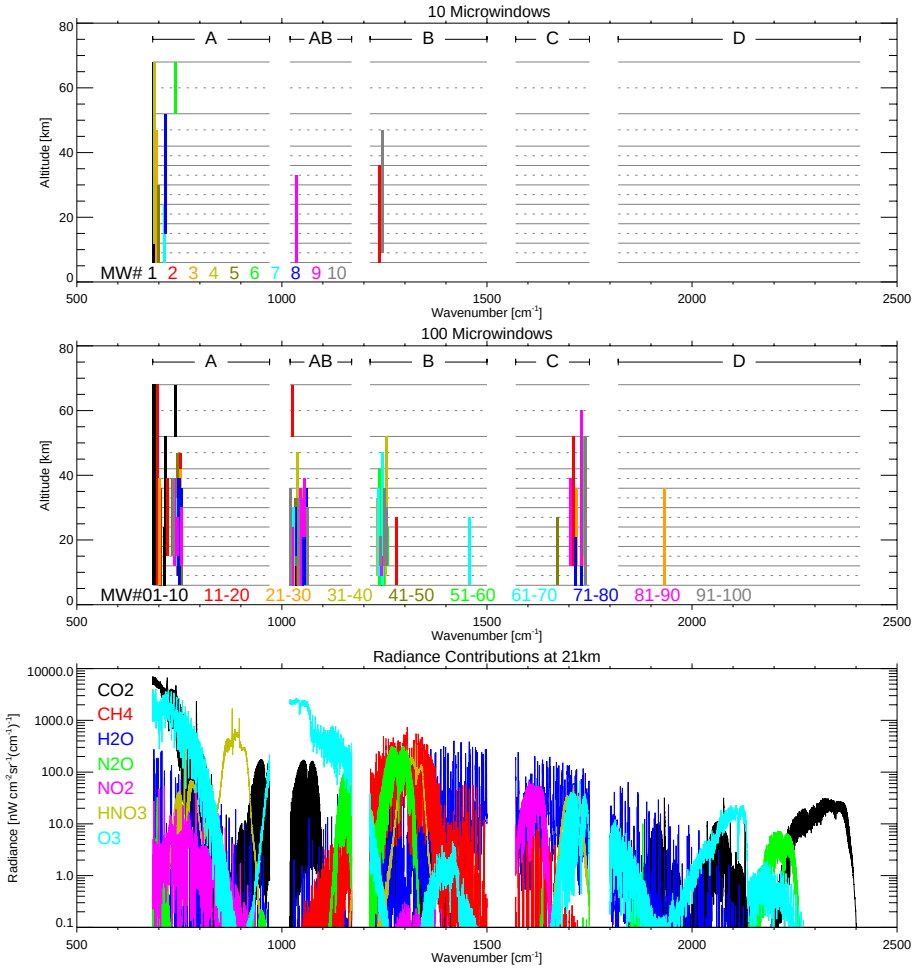

Figure 7: Location of the first 10 (top panel) and first 100 (middle) microwindows selected for this example. The lower panel shows the spectral features of the major contributing molecules within the MIPAS range.

While the first 10 microwindows are predominantly in the low wavenumber end of the A-band where the emission is mostly from CO_2, subsequent microwindows are clustered in different bands where CO_2 is only a secondary absorber (e.g., AB band) or where CH_4 (B band) or H_2O (C band) lines are used instead. Although there is a strong CO_2 feature in the D band (i.e., the 4.3μm CO_2 band) this is not used, probably due combination of low S/N, dense spectral structure and strong non-LTE effects.

Fig. 8 shows the growth in information, defined using either the random or total error covariance, as a function of the number of measurements used (one measurement being a spectral channel at a particular tangent height, so each microwindow can contain up to 121×17=2057 measurements, including masked points). As mentioned previously, the absolute definition of 'Information' depends on the choice of *a priori* covariance so the y-axis offset is not particularly significant. Even after 100 microwindows have been used, the accuracy continues to improve. However, the x-axis is logarithmic, clearly showing a diminishing return in information content per measurement (and therefore computation cost). After the second microwindow, the slope for both curves is almost constant which means that there is no obvious point at which to stop the selection. For the Off-Line processing, 7 *pT* microwindows are actually used (although not the same as those selected in this example — see Fig. 3.).

Fig. 10 shows the error budget after all 100 microwindows have been used. Comparing this with the result for the 7 microwindows used in the Off-Line retrieval (*cf* Fig. 4), in this case the total error is largely determined by the systematic error. Obviously the addition of more microwindows has reduced the random error but,

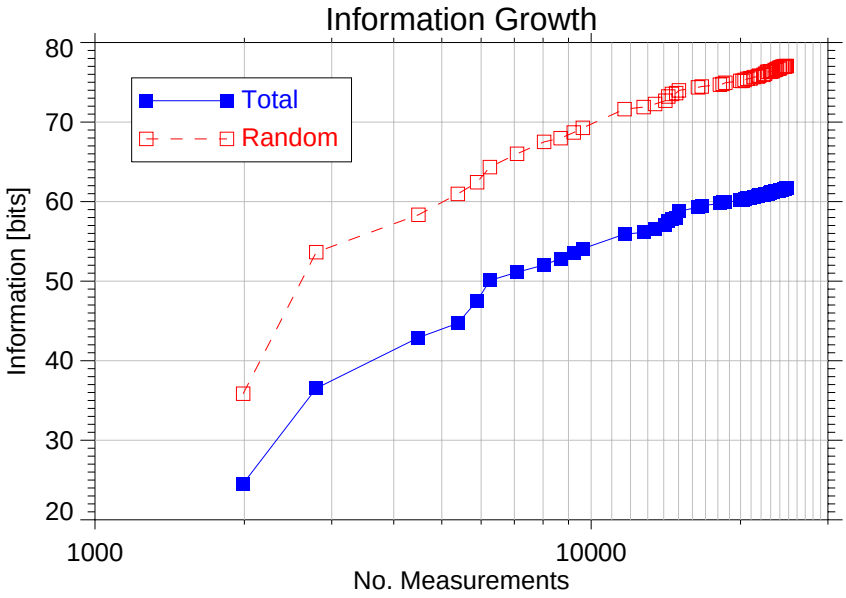

Figure 8: Growth in temperature information as microwindows (represented by the symbols) are added, with information defined either by just the random component of the retrieval error or the total retrieval error.

less intuitively, the systematic errors themselves have also been reduced. This arises from the combination of spectral masks and continuum retrieval which allows the selection algorithm some freedom to change the impact of the sign of the systematic errors in different microwindows, so achieving some cancellation.

4 Summary

The measurement domain for high spectral resolution limb-sounders is a two-dimensional space: tangent altitude v spectral channel. Channel selection for such instruments usually involves the use of 'microwindows', rectangular spaces within this domain. Traditionally this approach has been adopted to allow an atmospheric continuum and/or other uncertainties in 'baseline'-type features to be jointly retrieved for each microwindow and eliminated.

For MIPAS, while the retrievals themselves only consider the propagation of random measurement noise, the microwindow selection considers a number of additional sources of uncertainty in instrument characterisation and the forward model. By modelling the propagation of these errors through the retrieval, the various systematic error contributions to the retrieved products can be minimised and quantified.

The minimisation aspect is assisted by the use of the continuum retrieval as a sink for systematic errors and the imposition of of spectral masks to eliminate certain measurements within the microwindows.

These considerations have only been applied to maximising the information content of single profiles. However the systematic error budgets may provide some estimates on the spatial and temporal scales of various 'bias' components when profiles are combined.

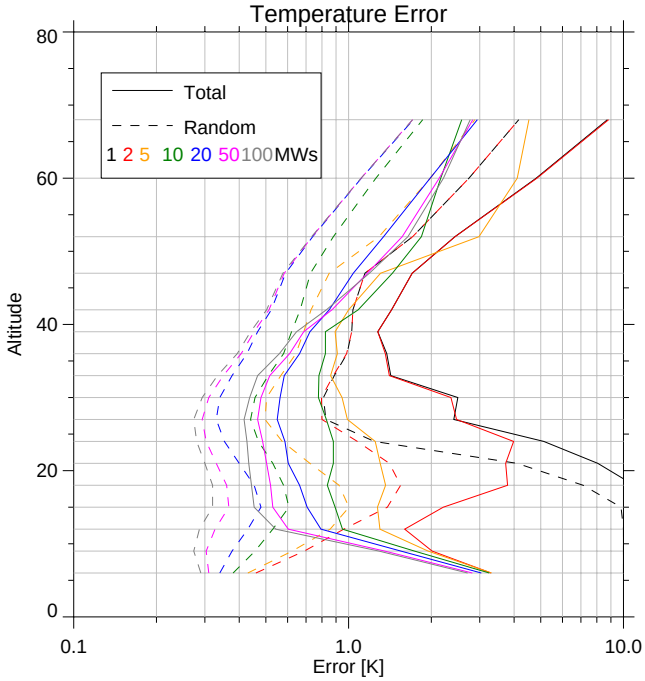

Figure 9: Improvement in the temperature retrieval Total Error (Accuracy) and Random Error (Precision) as more microwindows are added.

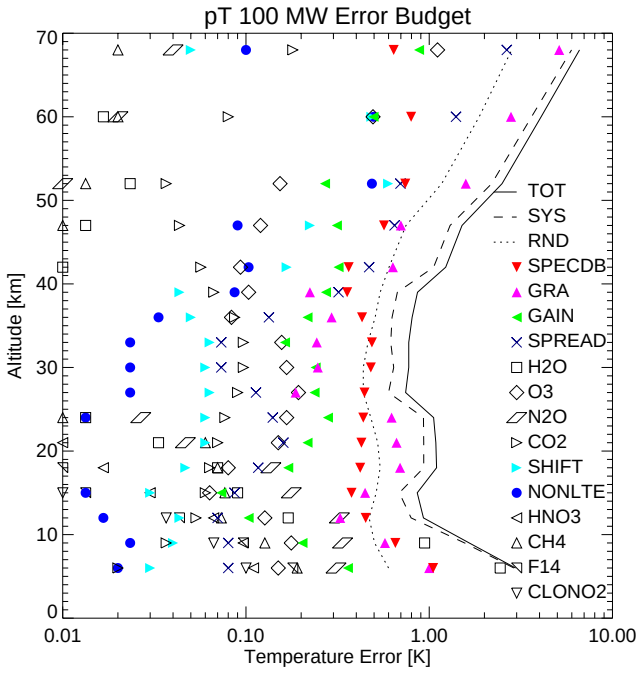

Figure 10: Error budget for the temperature component of the pT retrieval computed using 100 microwindows, for comparison with Fig. 4 showing the equivalent for the 7 microwindows used in the MIPAS Off-Line retrieval.

References

Dudhia, A., V. L. Jay and C. D. Rodgers (2002). Microwindow Selection for High-Spectral-Resolution Sounders. *App. Optics*, *41*, 3665–3673.

ESA (2000). Envisat-MIPAS: An Instrument for Atmospheric Chemistry and Climate Research. *ESA SP-1229*. ESTEC, Noordwijk, The Netherlands.

Ridolfi, M., B. Carli, M. Carlotti, T. von Clarmann, B. M. Dinelli, A. Dudhia, J-M. Flaud, M. Höpfner, P. E. Morris, P. Raspollini, G. Stiller and R. J. Wells (2000). Optimized Forward Model and Retrieval Scheme for MIPAS Near-Real-Time Data Processing. *App. Optics, 39*, 1323–1340.

Rodgers, C. D. (2000). *Inverse Methods for Atmospheric Sounding: Theory and Practice*. Singapore: World Scientific.